

# Short-Circuit Calculation of Power Systems with Penetration of Power Electronics Considering Converter Limitations

Jie Song, Marc Cheah-Mane, *Member, IEEE*, Eduardo Prieto-Araujo, *Senior Member, IEEE*,  
and Oriol Gomis-Bellmunt, *Fellow, IEEE*

**Abstract**—This paper deals with the challenge of short-circuit calculation for power systems populated with power electronics converters. A novel methodology has been presented to identify short-circuit equilibrium point of the studied system considering unbalanced voltage conditions and converter limitations. In particular, the studied system has been modeled with an element-based steady-state formulation. In particular, the equations of converters' operation, involves different control modes and various potential current-saturation states, are included. Then, an iterative approach has been proposed to identify the short-circuit equilibrium points that satisfies converters' limitation. Numerical case studies with VSCs prove that the proposed methodology can efficiently and accurately identify the equilibrium point even for studied system containing a large number of converters with different types and depths of short-circuit fault.

**Index Terms**—Short-Circuit Calculation, Voltage Source Converter, Current-Saturation, Unbalanced Fault.

## I. INTRODUCTION

Modern power systems are increasingly penetrated with power electronics converters as they are widely adopted in grid integration of renewable generation units and batteries as well as high-voltage direct current (HVDC) transmission, flexible AC transmission system (FACTS) and electrification of transportation. As a result, non-linear characteristics have been introduced with different control strategies of power converters, which should be included into the computational analysis of the studied system. In addition, the converter saturates current in case of overload or fault to protect semiconductor devices. Such current-saturation is especially critical for short-circuit calculation as several or all converters are likely to operate with a current-saturated state.

Short-circuit calculation is a fundamental but essential task in power system computational analysis. Short-circuit calculation of conventional power systems usually adopt Thévenin equivalent to represent the studied network at the fault location. However, this linearized grid equivalent representation fails to capture the operation of power converters. [IEC/IEEE standard].

Short-circuit analysis of power-electronics-dominated systems has been widely reported in the literature. [add references of short-circuit analysis/fault control using dynamic simulations.] The mentioned references are based on dynamic simulations. However, a steady-state computational analysis represents a more efficient approach for short-circuit calculation, especially for the studied system with a large number of converters.

Methodologies for short-circuit analysis considering power converters' operation have also been presented in the literature. [+Kaufman paper] models WT converters as current sources and presents an iterative approach to identify short-circuit equilibrium points considering converter current-limitation. However, the proposed methodology is limited to WT converter in PQ control and different control strategies *e.g.* grid-forming or PV control are not included. The authors of this paper proposed a comprehensive methodology that goes through all possible combinations of converters' current-saturation states and identifies short-circuit equilibrium points which satisfy converters' limitations. However, this methodology requires significantly high computing demand for the system with a large number of converters and therefore is limited for small-scale system. [+PV/offshore wind papers once they are available].

This paper presents a novel methodology for short-circuit calculation of power systems with penetration of power electronics. In particular, the contribution of this paper includes:

(to be completed)

## II. STEADY-STATE MODELING OF POWER SYSTEMS WITH PENETRATION OF POWER ELECTRONICS

### A. VSC Equivalent Model

The VSC regulates the power exchange with the AC grid at the Converter Connection Point (CCP) following the equivalent scheme shown in Fig. 1.

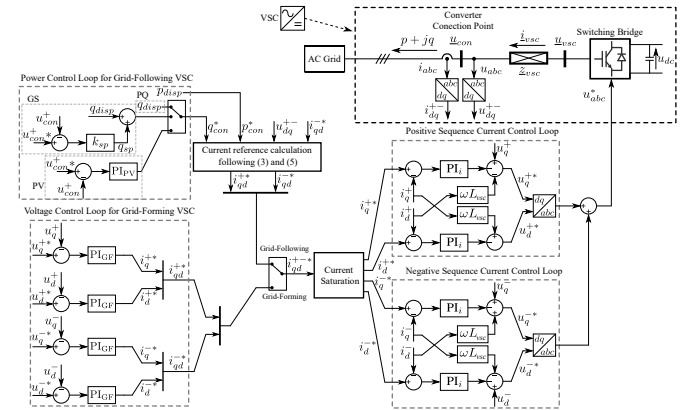


Fig. 1. VSC equivalent diagram and the control loop scheme (to be updated)

In this paper, the VSC is analyzed with a three-phase three-wire configuration as such configuration is widely adopted

in power engineering applications [1]. Therefore, the zero sequence element is equal to zero in VSC current injection with three-wire configuration, *i.e.*  $\underline{i}^0 = 0$ . Also, zero sequence voltage does not contribute to VSC power exchange with the AC grid and can be neglected at the CCP. However, the rest of the studied system can be analyzed in either three-wire or four-wire configurations. The positive and negative sequence elements of the CCP voltage,  $\underline{u}$ , and VSC current injection,  $\underline{i}$ , are expressed in a rectangular form and with a synchronous reference frame such that [2], [3]:

$$\begin{aligned}\underline{u} &= e^{j(\omega t + \theta_0)} \underbrace{(u_x^+ + j u_y^+)}_{\underline{u}^+} + e^{-j(\omega t + \theta_0)} \underbrace{(u_x^- + j u_y^-)}_{\underline{u}^-} \\ \underline{i} &= e^{j(\omega t + \theta_0)} \underbrace{(i_x^+ + j i_y^+)}_{\underline{i}^+} + e^{-j(\omega t + \theta_0)} \underbrace{(i_x^- + j i_y^-)}_{\underline{i}^-}\end{aligned}\quad (1)$$

where superscripts  $+$  and  $-$  respectively denote the positive and negative sequence elements, subscripts  $x$  and  $y$  respectively denote the real and imaginary part of a phasor,  $\omega$  is the nominal angular frequency of the studied system and  $\theta_0$  is the initial phase angle for the angular reference.

Then, the VSC active power exchange with the AC grid can be expressed as follows:

$$p = \underbrace{p_{con}}_{\bar{p}} + \underbrace{\cos(2\omega t + 2\theta_0)p_{cos} + \sin(2\omega t + 2\theta_0)p_{sin}}_{\tilde{p}} \quad (2)$$

where  $\bar{p}$  and  $\tilde{p}$  respectively denominate the constant and oscillating elements of the active power, and the three active power components can be expressed as:

$$\begin{cases} p_{con} = \underbrace{u_x^+ i_x^+ + u_y^+ i_y^+}_{\bar{p}_{con}} + \underbrace{u_x^- i_x^- + u_y^- i_y^-}_{\bar{p}_{con}} \\ p_{cos} = \underbrace{u_x^+ i_x^- + u_y^+ i_y^-}_{\bar{p}_{con}} + \underbrace{u_x^- i_x^+ + u_y^- i_y^+}_{\bar{p}_{con}} \\ p_{sin} = -\underbrace{u_x^+ i_y^- + u_y^+ i_x^-}_{\bar{p}_{con}} + \underbrace{u_x^- i_y^+ + u_y^- i_x^+}_{\bar{p}_{con}} \end{cases} \quad (3)$$

Similarly, the VSC reactive power with the AC grid can be expressed as:

$$q = \underbrace{q_{con}}_{\bar{q}} + \underbrace{\cos(2\omega t + 2\theta_0)q_{cos} + \sin(2\omega t + 2\theta_0)q_{sin}}_{\tilde{q}} \quad (4)$$

where the constant and oscillating reactive power elements can be expressed as:

$$\begin{cases} q_{con} = \underbrace{u_x^+ i_y^+ - u_y^+ i_x^+}_{\bar{q}_{con}} + \underbrace{u_x^- i_y^- - u_y^- i_x^-}_{\bar{q}_{con}} \\ q_{cos} = \underbrace{u_x^+ i_y^- - u_y^+ i_x^-}_{\bar{q}_{con}} + \underbrace{u_x^- i_y^+ - u_y^- i_x^+}_{\bar{q}_{con}} \\ q_{sin} = \underbrace{u_x^+ i_x^- + u_y^+ i_y^-}_{\bar{q}_{con}} - \underbrace{u_x^- i_x^+ + u_y^- i_y^+}_{\bar{q}_{con}} \end{cases} \quad (5)$$

Different control strategies can be adopted by the VSC to regulate the power exchange with AC grids, which results in different equations modeling the VSC operation. This paper presents the VSC equivalent model in grid-following mode (in particular PQ and PV control) and grid-forming mode as examples. In addition, the current-saturation scheme is employed in the VSC control as shown in Fig. 1, which results in different equations to model the VSC operation in various potential current-saturation states.

The VSC in PQ control manipulates the positive sequence current to regulate the constant elements in active and reactive power injections,  $p_{con}$  and  $q_{con}$ , following the reference value,

while the oscillating power elements,  $\tilde{p}$  and  $\tilde{q}$ , are not being controlled directly. The negative sequence current,  $\underline{i}^-$ , is set to zero in order to impose a symmetrical VSC current injection. In addition, current saturation must be implemented to VSC control in order to protect the converter from being overloaded as shown in Fig. 1. Therefore, VSC operation in PQ control can be divided into three current-saturation states (unsaturated-USS, partially saturated-PSS and fully saturated-FSS), which are expressed as follows:

$$\begin{cases} p_{con} = p_{ref}; q_{con} = q_{ref}; \underline{i}^- = 0 & \text{if USS} \\ q_{con} = q_{ref}; \underline{i}^+ = i_{vsc}^{\max}; \underline{i}^- = 0 & \text{if PSS} \\ p_{con} = 0; \underline{i}^+ = i_{vsc}^{\max}; \underline{i}^- = 0 & \text{if FSS} \end{cases} \quad (6)$$

where  $p_{ref}$  and  $q_{ref}$  are reference value for active and reactive power,  $i_{vsc}^{\max}$  is the VSC nominal current. The reactive power element is prioritized in current-saturated states. The power references can be defined either with constant dispatched values or with voltage-dependent varied values to include the grid-support scheme. In this paper, it is assumed that the VSC in PQ control tracks constant dispatched power references in normal operation. When the short-circuit fault happens, the reactive power controller output,  $i_{d0}$ , will be frozen and a voltage-droop grid support value will be added following the grid codes. The frozen value,  $i_{d0}$ , is depending on the pre-fault operation point of the studied system and is considered as a known constant in this paper for short-circuit calculation. Then, the power references for the VSC in PQ control can be expressed as follows:

$$\begin{cases} p_{ref} = p_{disp}; q_{ref} = q_{disp} & \text{if fault} = 0 \\ p_{ref} = p_{disp}; q_{ref} = u^+ [i_{d0} + k_{sp}(u_{ref-gs} - u^+)] & \text{if fault} = 1 \end{cases} \quad (7)$$

where  $p_{disp}$  and  $q_{disp}$  are dispatched values of active and reactive power,  $k_{sp}$  is the voltage-droop gain of grid-support current and  $u_{ref-gs}$  is the positive sequence voltage reference for grid-support control during the fault.

The VSC in PV control also tracks a dispatched value for the constant element of active power,  $p_{con}$ , while the constant element of reactive power element,  $q_{con}$ , is adjusted to maintain a constant positive sequence voltage magnitude in positive sequence such that:

$$\begin{cases} p_{con} = p_{disp}; u^+ = u_{ref-PV}; \underline{i}^- = 0 & \text{if USS} \\ u^+ = u_{ref-PV}; \underline{i}^+ = i_{vsc}^{\max}; \underline{i}^- = 0 & \text{if PSS} \\ p_{con} = 0; \underline{i}^+ = i_{vsc}^{\max}; \underline{i}^- = 0 & \text{if FSS} \end{cases} \quad (8)$$

where  $u_{ref-PV}$  is the positive-sequence voltage magnitude reference at CCP for the VSC in PV control. The reactive current element in positive sequence (which is corresponding to voltage control) is prioritized in PSS over the active current.

The grid-forming VSC imposes a symmetrical voltage following the reference value in normal operation. When being saturated, the grid-forming VSC can be represented as a current source which imposes a symmetrical current at the nominal current magnitude. In addition, a frequency droop scheme is adopted by the grid-forming converter to implement a distributed slack for power-sharing purpose whether the converter is saturated or not. The partially saturated state (PSS) is not applied to the grid-forming VSC as it does not directly regulate the active or reactive power elements. Therefore, the

grid-forming VSC operation can be divided into two current-saturation states (USS and FSS) as follows:

$$\begin{cases} u^+ = u_{ref-GF}; \underline{u}^- = 0; & \text{if USS} \\ i^+ = i_{vsc}^{\max}; \underline{i}^- = 0; & \text{if FSS} \end{cases} \quad (9)$$

where  $u_{ref-GF}$  is the positive sequence voltage magnitude reference for the grid-forming VSC.

It should be noticed that different options can be adopted for VSC control in different applications. For example, the active power elements can be prioritized for a grid-following converter in a current-saturated state; the converter in PQ control can inject negative sequence current and regulate the oscillating power elements; in the studied system with multiple grid-forming units, they can use frequency as the communication signal for power-sharing purpose. These different options are not explicitly expressed in this paper for the sake of simplicity. The methodology for short-circuit calculation proposed in this paper can be equally applied for other options of VSC control by including the corresponding equivalent model of converter operation into the studied system formulation.

#### B. A Practical VSC Equivalent Model for Efficient Short-Circuit Calculation

The VSC equivalent model presented in the previous Section could accurately formulate the converter operation in different control modes and various potential current-saturation states. However, the presented model cannot be adopted directly for short-circuit calculation as usually the current-saturation state of a converter in a specific short-circuit fault scenario is uncertain. Therefore, it is not clear which equation should be selected to model the converter's operation. A generic approach is to traverse all possible combinations of converters' current-saturation states and to identify the short-circuit equilibrium point that satisfying converters' operation limits. However, this approach is not feasible for a studied system containing a large number of converters as it is computational burdensome (e.g. a system with 20 grid-following converters yields  $3^{20} = 3.49 \times 10^9$  combinations, which is impossible to sweep all of them in a feasible time).

This paper proposes an iterative methodology for efficient short-circuit calculation, which is presented later in Section III. In particular, the converters' set points are updated for each iteration,  $k$ , based on the solution obtained from the previous iteration,  $k-1$ . Therefore, the VSC equivalent model is revised in order to incorporate with the proposed iterative solver.

1) *Grid-Following Converter*: The grid-following converter is modeled as a current source for both PQ and PV control. In particular, the grid-following converter does not inject negative or zero sequence current following the equivalent model in the previous Section. Therefore, the grid-following converter is modeled as a current source that inject zero current for negative and zero sequence whether the converter is saturated or not:

$$i_x^- + ji_y^- = i_x^0 + ji_y^0 = 0 \quad (10)$$

The positive sequence current injection for a grid-following converter is defined in  $qd$  frame where  $q$  and  $d$ -axis elements

are respectively corresponding to active and reactive current, such that:

$$i_q^+ + ji_d^+ = (i_x^+ + ji_y^+)e^{j\theta_{u^+}} \quad (11)$$

where  $\theta_{u^+}$  is the phase angle of the positive voltage at the converter connection point,  $\underline{u}^+$ . The reference value of the positive sequence current injection for the converter in PQ control can be calculated iteratively as follows:

$$\begin{cases} i_{q-ref(k)}^+ = p_{ref(k-1)}/u_{(k-1)}^+ \\ i_{d-ref(k)}^+ = q_{ref(k-1)}/u_{(k-1)}^+ \end{cases} \quad (12)$$

where  $i_{q-ref(k)}^+$  and  $i_{d-ref(k)}^+$  are positive sequence active and reactive current references for iteration  $k$ ,  $u_{(k-1)}^+$  is the positive sequence CCP voltage magnitude obtained from iteration  $k-1$ ,  $p_{ref(k-1)}$  and  $q_{ref(k-1)}$  are active and reactive power references obtained from iteration  $k-1$ . In particular, the active power reference,  $p_{ref(k-1)}$ , is defined with a constant dispatched value, which is the same for all iterations. While the reactive power reference is modified in each iteration in order to include the grid-support scheme during the fault such that:  $q_{ref(k-1)} = u_{(k-1)}^+ [i_{d0} + k_{sp}(u_{ref-gs} - u_{(k-1)}^+)]$ .

The positive sequence active current reference for the converter in PV control,  $p_{ref}$ , is the same as the converter in PQ control as expressed in (12) while reactive current reference,  $q_{ref}$ , will be calculated iteratively to achieve the reference voltage in positive sequence such that:

$$\begin{cases} i_{q-ref(k)}^+ = p_{ref(k-1)}/u_{(k-1)}^+ \\ i_{d-ref(k)}^+ = i_{d-ref(k-1)}^+ + (u_{ref-PV} - u_{(k-1)}^+)/z_{eq}^+ \end{cases} \quad (13)$$

where  $z_{eq}^+$  is the positive sequence grid equivalent impedance. The authors of this paper have investigated on the grid impedance for different voltage levels considering the operation of power electronics [4]. In this paper, the grid equivalent impedance is assumed as unvaried and is given as a known constant for the sake of simplicity.

In addition, the current references obtained from (12) and (13) will be modified when the current-saturation is triggered in respect to the converter's current limitation. Therefore, the actual positive sequence current injections from the grid-following converter for iteration  $k$  can be expressed as follows:

$$\begin{cases} i_{q(k)}^+ = i_{q-ref(k)}^+; i_{d(k)}^+ = i_{d-ref(k)}^+ & \text{if } |i_{q-ref(k)}^+ + ji_{d-ref(k)}^+| \leq i_{vsc}^{\max} \text{ USS} \\ i_{q(k)}^+ = \text{sign}(i_{q-ref(k)}^+) \sqrt{i_{vsc}^{\max 2} - i_{d-ref(k)}^+{}^2}; i_{d(k)}^+ = i_{d-ref(k)}^+ & \text{if } |i_{q-ref(k)}^+ + ji_{d-ref(k)}^+| \leq i_{vsc}^{\max} \& |i_{q-ref(k)}^+| \leq i_{vsc}^{\max} \text{ PSS} \\ i_{q(k)}^+ = 0; i_{d(k)}^+ = \text{sign}(i_{d-ref(k)}^+) i_{vsc}^{\max} & \text{if } |i_{q-ref(k)}^+ + ji_{d-ref(k)}^+| \leq i_{vsc}^{\max} \& |i_{q-ref(k)}^+| > i_{vsc}^{\max} \text{ FSS} \end{cases} \quad (14)$$

2) *Grid-Forming Converter*: The grid-forming converter can be modeled as a current source that injects zero current for zero sequence such that:  $i_x^0 + ji_y^0 = 0$ . While for positive and negative sequence, it can be modeled as a voltage source or a current source depending on its current-saturation states, which can be expressed as follows:

$$\begin{cases} u_{(k)}^+ = u_{ref-GF}; \underline{u}_{(k)}^- = 0; & \text{if USS} \\ i_{(k)}^+ = i_{vsc}^{\max}; \underline{i}_{(k)}^- = 0; & \text{if FSS} \end{cases} \quad (15)$$

The current-saturation state of a grid-forming converter can be updated based on the solution obtained from the current iteration,  $k - 1$ , as the evidence to select the equations modeling the converter operation in the upcoming iteration,  $k$ , such that:

$$sta_k = \begin{cases} \text{USS} & \text{if } i_{(k-1)}^{a,b,c} \leq i_{vsc}^{\max} |u_{(k-1)}^{\text{ph}}| \geq u_{\text{ref}}^{\text{ph}} \forall \text{ph} \in [a, b, c] \\ \text{FSS} & \text{if } i_{(k-1)}^{\text{ph}} > i_{vsc}^{\max} \forall \text{ph} \in [a, b, c] \end{cases} \quad (16)$$

### C. Formulation of Power Systems with penetration of power electronics for Short-Circuit Calculation

to be filled.

Admittance matrix plus current source/voltage source equivalent model of converters.

### III. IDENTIFICATION OF SHORT-CIRCUIT EQUILIBRIUM POINT

A methodology for short-circuit calculation is developed based on the VSC equivalent model expressed in previous sections. In particular, equations modeling the converters' operation will be updated iteratively in order to obtain the short-circuit equilibrium point that satisfies converters' operation limits.

The methodology for short-circuit calculation is summarized as shown in Algorithm 1. The required input information includes the admittance matrix of the studied system circuit,  $\mathbf{Y}$ , the set of equations modeling the operation of power electronics and non-power electronics elements,  $H$ , the vector of initial current references for grid-following converters (if any),  $I_{ref0}$ , the vector of initial states of grid-forming converters (if any),  $sta_0$ , the maximum iteration number,  $K_{\max}$ , and the error tolerance,  $\epsilon$ .

The calculation starts with the initial current reference values for grid-following converters,  $I_{ref0}$ , and the initial current-saturation states of grid-forming converters,  $sta_0$ . The set of equations,  $H$ , is defined with the converters' set points. The system of equations modeling the studied system,  $SE$ , is updated and solved for each iteration  $k$ . Then, the obtained solution,  $sol$ , is utilized to update converter set points and the resulted equations formulating the studied system for the next iteration following the equivalent model expressed in Section II-B. In particular, the current reference values are calculated as expressed in (12), (13) and (14) for all grid-following converters. The current-saturation stats of grid-forming converters are updated as expressed in (16), which results in different equations modeling the converters' operation in the upcoming iteration. The calculation algorithm will be performed till convergence or the maximum iteration number has been achieved.

### IV. CASE STUDIES

#### A. PQ converter

Short-circuit with the fault impedance of  $z_{sc} = j0.001$  pu and tested with different types of fault:

#### Algorithm 1: Identification of Short-Circuit Equilibrium Point

**input :** Admittance matrix  $\mathbf{Y}$ , Set of equations  $H$ , initial current references for grid-following converter  $I_{ref0}$ , initial states for grid-forming states,  $sta_0$ , maximum iteration number  $k_{\max}$   
**output:** Identified equilibrium (eq.) point  $EP$

```

 $k = 0;$ 
 $I_{ref} = I_{ref0}; sta = sta_0;$ 
begin
  for  $k \leftarrow 1$  to  $k_{\max}$  do
    define  $H$  with  $I_{ref}$  and  $sta$ ;
    // define converters equations with given references
     $SE := [\mathbf{Y}, H];$  // define system equations
     $sol = f_{solve}(SE_f);$ 
    if  $k > 1$  then
      foreach  $d \in [1, D]$  &  $s \in \{+, -, 0\}$  do
         $\Delta u_d^s = |u_{d(k)}^s - u_{d(k-1)}^s|;$ 
      end
    end
    if  $\Delta u_d^s < \epsilon \forall d \in [1, D]$  and  $s \in \{+, -, 0\}$  then
       $EP = sol;$  break;
      // converged
    end
    update  $I_{ref}$  with  $sol$  following (12), (13) and (14);
    update  $sta$  with  $sol$  following (16);
  end
  return 'No Equilibrium Point';
end

```

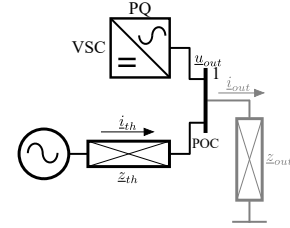


Fig. 2. Scheme1

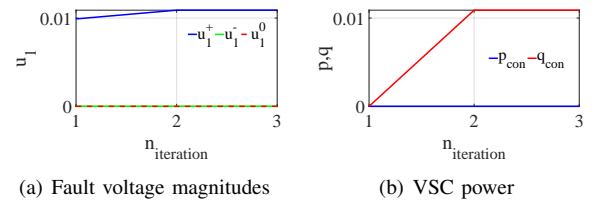


Fig. 3. PQ-3P2G

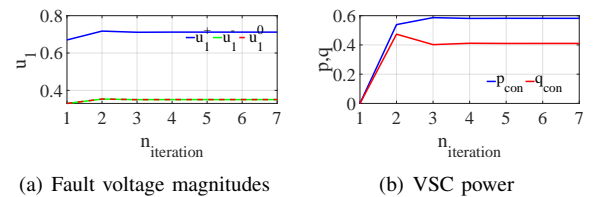


Fig. 4. PQ-1P2G

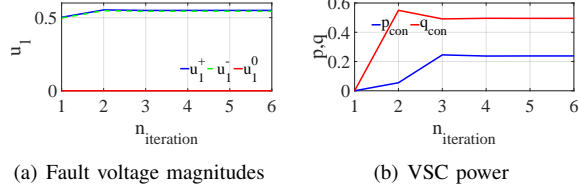


Fig. 5. PQ-P2P

### B. PV converter

Fault impedance of  $z_{sc} = j1$  pu and tested with different types of fault. (the algorithm also works for lower fault impedance, and it always converged in 3 iterations, like PQ converter with 3P2G fault).

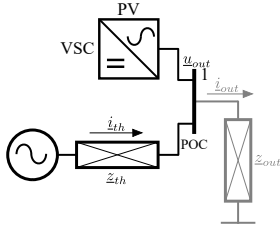


Fig. 6. Scheme1

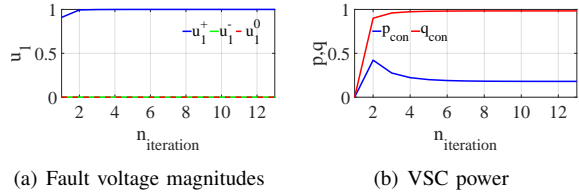


Fig. 7. PV-3P2G

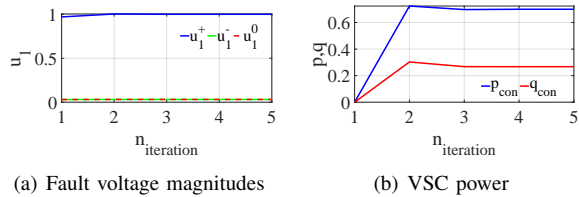


Fig. 8. PV-1P2G

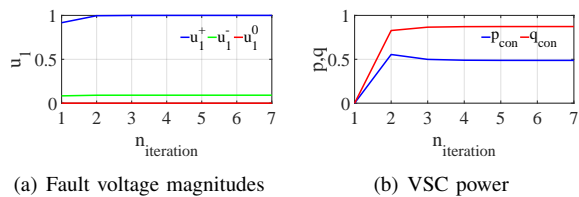


Fig. 9. PV-P2P

### C. Case 1 + Experimental Validation

### D. Case 2

### REFERENCES

- [1] M. Z. Kamh and R. Iravani, "Unbalanced model and power-flow analysis of microgrids and active distribution systems," *IEEE Transactions on Power Delivery*, vol. 25, no. 4, pp. 2851–2858, 2010.
- [2] P. S. Kundur, "Power System Stability and Control," 1994.
- [3] R. A. Flores, I. Y. Gu, and M. H. Bollen, "Positive and Negative Sequence Estimation for Unbalanced Voltage Dips," *2003 IEEE Power Engineering Society General Meeting, Conference Proceedings*, vol. 4, pp. 2498–2502, 2003.
- [4] O. Gomis-Bellmunt, J. Song, M. Cheah-Mane, and E. Prieto-Araujo, "Steady-state impedance mapping in grids with power electronics: What is grid strength in modern power systems?," *International Journal of Electrical Power & Energy Systems*, vol. 136, p. 107635, 3 2022.